Human Molecular Genetics, 2004, Vol. 13, No. 2 **159–170**
DOI: 10.1093/hmg/ddh019
Advance Access published on November 25, 2003

Mutant presenilins specifically elevate the levels of the 42 residue β-amyloid peptide *in vivo*: evidence for augmentation of a 42-specific γ secretase

Joanna L. Jankowsky[1,†], Daniel J. Fadale[3], Jeffrey Anderson[4], Guilian M. Xu[1], Victoria Gonzales[1], Nancy A. Jenkins[5], Neal G. Copeland[5], Michael K. Lee[1], Linda H. Younkin[3], Steven L. Wagner[4,6], Steven G. Younkin[3] and David R. Borchelt[1,2,*]

[1]Department of Pathology and [2]Department of Neuroscience, The Johns Hopkins University School of Medicine, Baltimore, MD 21205, USA, [3]Mayo Clinic Jacksonville, 4500 San Pablo Road, Jacksonville, FL 32224, USA, [4]Merck Research Labs, San Diego, 505 Coast Boulevard South, La Jolla, CA 92037, USA, [5]Mouse Cancer Genetics Program, NCI-Frederick Cancer Research and Development Center, Frederick, MD 21702, USA and [6]Neurogenetics Inc., 11085 North Torrey Pines Road, Suite 300, La Jolla, CA 92037, USA

Received August 15, 2003; Revised and Accepted November 11, 2003

Amyloid precursor protein (APP) is endoproteolytically processed by BACE1 and γ-secretase to release amyloid peptides (Aβ40 and 42) that aggregate to form senile plaques in the brains of patients with Alzheimer's disease (AD). The C-terminus of Aβ40/42 is generated by γ-secretase, whose activity is dependent upon presenilin (PS 1 or 2). Missense mutations in PS1 (and PS2) occur in patients with early-onset familial AD (FAD), and previous studies in transgenic mice and cultured cell models demonstrated that FAD-PS1 variants shift the ratio of Aβ40 : 42 to favor Aβ42. One hypothesis to explain this outcome is that mutant PS alters the specificity of γ-secretase to favor production of Aβ42 at the expense of Aβ40. To test this hypothesis *in vivo*, we studied Aβ40 and 42 levels in a series of transgenic mice that co-express the Swedish mutation of APP (APPswe) with two FAD-PS1 variants that differentially accelerate amyloid pathology in the brain. We demonstrate a direct correlation between the concentration of Aβ42 and the rate of amyloid deposition. We further show that the shift in Aβ42 : 40 ratios associated with the expression of FAD-PS1 variants is due to a specific elevation in the steady-state levels of Aβ42, while maintaining a constant level of Aβ40. These data suggest that PS1 variants do not simply alter the preferred cleavage site for γ-secretase, but rather that they have more complex effects on the regulation of γ-secretase and its access to substrates.

INTRODUCTION

The pathology of Alzheimer's disease (AD) is characterized by amyloid lesions formed by aggregated peptides (β-amyloid, Aβ), which are derived from the amyloid precursor protein (APP) through endoproteolytic cleavage by BACE1 and γ-secretase. APP is also a substrate for other endoproteases (α-secretase and BACE2), and collectively these cleavages generate a range of amyloid (Aβ) peptides (for review see 1). The most pathogenic of these peptides, Aβ40 and 42, share a common N-terminus (+1) and differ by two residues at their C-terminus (2–7). Mutations in APP identified from familial AD (FAD) kindreds alter the protein's normal processing, causing either increased production of both peptides or a specific elevation in Aβ42 (8–11). The longer Aβ42 peptide is more prone than Aβ40 to aggregate *in vitro* (12,13), and is the

*To whom correspondence should be addressed at: Department of Pathology, The Johns Hopkins University School of Medicine, 558 Ross Research Building, 720 Rutland Ave, Baltimore, MD 21205, USA. Tel: +1 4105025174; Fax: +1 4109559777; Email: drbor@jhmi.edu.
[†]Present address:
Division of Biology, MC 156-29 California Institute of Technology, Pasadena, CA 91125, USA.

major species detected immunocytochemically in the brains of AD patients (14).

Mutations in two additional genes, presenilin 1 (PS1) and its homolog PS2, also cause early-onset FAD (15–17). Studies in both vertebrates and invertebrates suggest that PS1 and PS2 are components of a larger protein complex that contains nicastrin, Aph-1, and PEN-2 (18–27). This complex is either a required cofactor for, or is itself, the γ-secretase activity that generates the C-termini of Aβ40 and 42 (19,22–24,28–35). Deletion of both PS1 and PS2 leads to a complete loss of γ-secretase activity (33). Cells deficient in PS1 also show abnormalities in the subcellular trafficking of integral membrane proteins, including APP (36,37).

An interaction between the presenilins and APP was first suggested by the observation that the plasma of patients with mutations in PS1 had higher ratios of Aβ42 relative to Aβ40 than patients with sporadic AD (38). Subsequent work in cell models demonstrated that co-expression of FAD-mutant PS1 with APP reproduced the rise in Aβ42 relative to Aβ40 that had been seen in patients with PS1-associated AD (39–41). This shift in Aβ40 : Aβ42 ratio was also found in the brains of transgenic mice co-expressing one of several FAD PS1 mutations (M146V, M146L, A246E or M286L) with the Swedish mutation of APP (39,42–44). Similar shifts in the steady-state ratios of mouse Aβ40 : Aβ42 were also noted in mice expressing only FAD-variant PS1 (45) or PS2 (46). Transgenic mice co-expressing mutated PS1 and APP developed amyloid pathology much earlier than mice expressing only APP; the acceleration in amyloid formation directly correlated with the change in the Aβ40 : Aβ42 ratios (42,47,48). In contrast, co-expression of wild-type human PS1 with mutant human APP had no impact on the rate of amyloid formation (44).

Studies of dominant negative versions of PS1 and chemical inhibitors of γ-secretase have been interpreted as evidence that PS1 may comprise the active site of the γ-secretase complex (28,31,49–52). Moreover, because some of these inhibitors coordinately depress both Aβ40 and Aβ42 production, it has been assumed that one enzyme complex is responsible for the production of both peptides (50,51). In such a setting, FAD mutations in PS1 might alter the ratio of Aβ peptides produced from APP simply by shifting the specificity of γ-secretase to favor cleavage at residue 42 over that at 40. In this scenario, mutations that increase the output of Aβ42 should be accompanied by a decrease in the generation of Aβ40.

In the current work, we took advantage of recent advances in ELISA methodology to examine Aβ40 and Aβ42 levels in several lines of APPswe mice co-expressing either of two FAD PS1 variants (A246E and dE9). Each PS1 variant accelerated the rate of amyloid deposition to differing extents. After quantifying the levels of Aβ40 and Aβ42 in the brains of young, pre-symptomatic animals, we found that co-expression of either PS1A246E or PS1-dE9 in APPswe transgenic mice specifically increased Aβ42 levels without altering Aβ40. From these data, we defined a direct correlation between the age of amyloid onset and Aβ42 levels. Based on work from cultured cell models suggesting that mutant PS1 alters the production of Aβ42 (39–41), we conclude that changes in the steady-state level of this peptide in our transgenic mice were most likely due to alterations in the processing of APP. We suggest that FAD-PS1 variants may increase the accessibility of BACE1-cleaved C-terminal fragments of APP (β-CTFs) to a γ-secretase that preferentially cleaves at residue 42.

RESULTS

Transgene-derived APPswe expression in lines Q2-2, 85 and C3-3

In this study, we used three different lines of mice that express Mo/HuAPP695swe under control of the mouse prion protein promoter (53). The Mo/Hu APP695swe construct encodes mouse sequence throughout the extra- and intracellular regions, human sequence within the Aβ domain, and Swedish mutations K594N/M595L just prior to the Aβ N-terminus. Lines Q2-2 and C3-3 harbor only the APPswe construct and have been previously characterized (53). The third line of APPswe mice used for this study, line 85, expresses an identical Mo/Hu APPswe construct in conjunction with the exon-9-deleted variant of human presenilin 1 (PS1-dE9) (54). This line was produced by co-injection of the APPswe and PS1-dE9 vectors, each controlled by its own prion promoter element, following previously reported procedures (55).

Immunoblot analysis of brain protein separated by SDS–PAGE demonstrated relatively high levels of APPswe expression in each of these lines (Fig. 1). Blots probed with monoclonal antibody 22C11, which detects a shared epitope in the N-terminal region of mouse and human APP, showed that each of the transgenic lines expresses 2- to 4-fold more total APP than non-transgenic animals (Fig. 1B). Immunoblots probed with monoclonal antibody 6E10, which detects the humanized Aβ domain of our transgene product, demonstrated that APPswe protein levels were highest in the brains of mice from line C3-3; overall expression in the three lines ranked Q2-2 < 85 < C3-3 (Fig. 1A).

PS1-A246E and PS1-dE9 possess different amyloidogenic potentials

In previous studies we (44,47) and others (42,43,48) have shown that the co-expression mutant PS1 with APPswe can accelerate the rate of amyloid deposition. By contrast, co-expression of wild-type human PS1, even at very high levels, has no effect on the rate of amyloid deposition (44). Here we extend this work to compare the effects of two FAD PS1 variants which hasten amyloid onset to differing degrees. As shown previously (47), transgenic mice from line C3-3 do not develop amyloid deposits until well beyond 18 months of age (Fig. 2A–C). Co-expression of PS1-A246E (line N-5) halves this time, with C3-3/N-5 mice developing amyloid deposits by 9–12 months (Fig. 2D–F) (47). Plaque burden in the C3-3/N-5 mice worsens with age, and by 20–24 months the hippocampus and cortex show high amyloid burdens. A similar acceleration in amyloid deposition has been noted when mice from a different line of PS1-A246E (line I2-4) are crossed to C3-3 mice (44). When mice from line C3-3 are crossed with mice expressing the exon-9-deleted variant of PS1 (line S-9) (56), substantial amyloid deposition is visible by 6 months of age (Fig. 2G) (57). As with PS1-A246E, amyloid burdens in the C3-3/PS1-dE9 mice increase throughout life

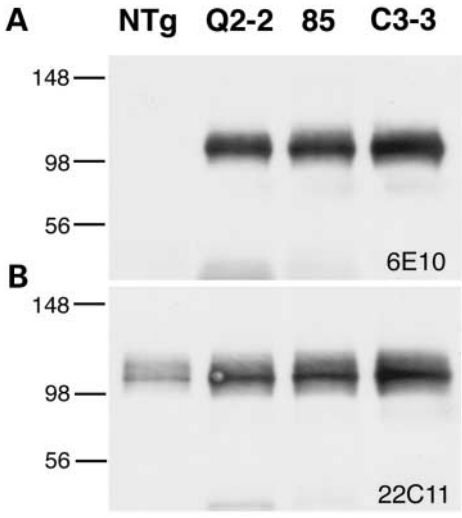

Figure 1. Transgene-derived APPswe expression in the three mouse lines studied. (**A**) Human-Aβ-specific antibody 6E10 was used to detect transgene-derived APP in brain homogenates from line Q2-2, 85 and C3-3 animals. (**B**) Antibody 22C11 was used to detect endogenous mouse APP and amyloid precursor-like protein 2 (APLP-2) (80) in non-transgenic controls and both endogenous APP/APLP-2 and transgene-derived human APPswe in lines Q2-2, 85 and C3-3. Immunoblot analysis consistently revealed the highest APPswe expression in line C3-3, the lowest in line Q2-2, with Line 85 falling between the two lines.

(Fig. 2H and I). The early appearance of amyloid deposits was observed in offspring of C3-3 mice mated with two different lines of PS1-dE9 mice (line S-9 shown here and line O-7, data not shown), confirming that the effect was due to the PS1-dE9 transgene and not to an artifact of integration site.

Measurements of Aβ levels by immunoprecipitation with antibodies to the N-terminus of Aβ followed by immunoblotting with antibodies specific for the 40 or 42 termini demonstrated that the ratio of Aβ40 : Aβ42 varied by genotype (Fig. 3A). In mice expressing only APPswe the ratio was ~3 : 1; co-expressing PS1A246E decreased the ratio to ~1.75 : 1, and co-expressing PS1dE9 dropped the ratio to ~0.75 : 1. The degree of change in Aβ40 : Aβ42 ratios was proportional to the acceleration in Aβ deposition across genotypes (Fig. 3B).

Further evidence of the highly pathogenic activity of PS1-dE9 was seen when we extended our study to mice that express lower levels of APPswe. Mice from line Q2-2 do not develop amyloid pathology until after 20 months of age (Fig. 4A and E). To test whether co-expression of mutant PS1 could induce plaques in this non-depositing line, we crossed Q2-2 APPswe mice with animals expressing either PS1-A246E (line I2-4) (44,56) or PS1-dE9 (line S-9) (56,57). Despite its ability to accelerate amyloid deposition in line C3-3 mice (44), co-expression of PS1-A246E in line Q2-2 produced no amyloid pathology in any brain region through 20 months of age (Fig. 4B and F). In contrast, double transgenic offspring from Q2-2 × PS1-dE9 developed substantial amyloid pathology by mid-life (Fig. 4C and G). Deposits probably began at 15–18 months; by the time they were sacrificed at 20 months, animals had a considerable burden of both diffuse and compact plaques throughout the hippocampus and cortex. Thus, PS1-dE9 consistently induces earlier pathology in APPswe transgenic mice than PS1-A246E, and is pathogenic enough to cause amyloid formation even in a line of APPswe animals that would otherwise have remained free of deposits.

Analysis of the double-transgenic mice, created by co-injecting Mo/Hu APPswe and PS1-dE9 constructs, again confirmed the amyloidogenic potential of the PS1-dE9 variant. Animals from line 85 express levels of APPswe intermediate to lines C3-3 and Q2-2 (Fig. 1); however, because they invariably co-express PS1dE9, line 85 mice develop amyloid deposits far earlier than either single transgenic APPswe line (Fig. 4D and H). Occasional deposits can be found in line 85 mice as young as 6 months of age, and by 9 months most animals have a significant plaque burden in the cortex and hippocampus (Fig. 4D and H). Thus the dE9 variant appears to be a highly pathogenic mutation, with profound effects on the deposition of amyloid peptides. Despite its highly pathogenic activity, expression of PS1-dE9 alone in mice is not sufficient to induce amyloid deposits from endogenous mouse APP (not shown), consistent with previous reports of other FAD variant PS1 transgenic mice (48).

Mutant PS1 specifically increases the steady-state levels of Aβ42

By two independent approaches, we have demonstrated that the earlier appearance of amyloid in mice co-expressing APPswe (line C3-3) with PS1-A246E (line N-5) or PS1-dE9 (line S-9) is associated with a change in the ratio of Aβ40 : Aβ42 to favor Aβ42 (Fig. 3) (39). In both of these studies, however, variance in the efficiency of Aβ peptide captured by either immunoprecipitation or ELISA made it difficult to distinguish whether Aβ42 levels were increased at the expense of Aβ40, or whether the level of Aβ42 increased independently while Aβ40 remained unchanged. In the course of our study, a refined ELISA approach (58) was developed that allowed us to address this issue.

Using the refined ELISA assay, we studied the levels of Aβ peptides in the brains of young, pre-deposit animals from each of the double transgenic lines described above (Fig. 5). Tissue was processed using a two-step extraction method: following sonication in 0.2% diethylamine (DEA) and high-speed centrifugation, soluble Aβ was recovered in the supernatant, and the pellet was then re-extracted with 70% formic acid (FA) to recover all remaining insoluble species. The two fractions were assayed separately; data for total Aβ were calculated by addition of the DEA and FA fraction values obtained for each animal. We noted that approximately 50% of Aβ40 was extracted by DEA, while a lower, and more variable, percentage of Aβ42 was extracted by this solvent (Table 1). Because all of the samples were prepared from young, pre-deposit animals, especially in the case of the mice transgenic for only APPswe, we do not believe that the relative insolubility of Aβ42 was due to oligomerization of this peptide, but rather to an inherent difference in the solubility of the two peptides in DEA. Our comparisons across genotypes in each transgenic series therefore focus on total Aβ values rather than DEA- or FA-soluble fractions to accommodate the differential solubility of the two peptides.

Two separate series of experiments were performed. In one series we compared Aβ40 and Aβ42 levels in the brains of

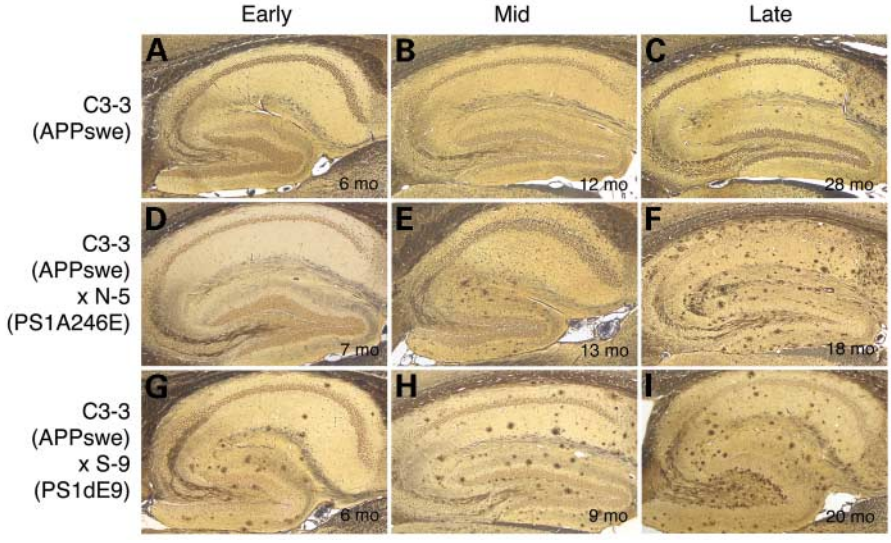

Figure 2. Co-expression of PS1-dE9 dramatically accelerates amyloid pathology in APPswe transgenic mice. (**A–C**) Mice transgenic for only APPswe (line C3-3) develop hippocampal amyloid deposits at very late ages as shown by Hirano silver stain. Amyloid plaques are absent from young (A) and middle-aged (B) animals, appearing only in mice over 20 months of age (C). (**D–F**) Co-expression of PS1-A246E accelerates the appearance of amyloid plaques. Deposits are first observed in line C3-3 APPswe/PS1-A246E double transgenic mice at 10–13 months of age (E) before plaque load worsens with age (F). (**G–I**) Co-expression of PS1-dE9 in line C3-3 APPswe mice further hastens the appearance of pathology. Double transgenic APPswe/PS1-dE9 mice have a substantial number of deposits by 6 months of age (G), and plaque burden increases progressively with time (H and I). The hippocampus is shown in all panels for ease of comparison; plaques are also observed in superficial layers of the anterior cortex concurrent with hippocampal onset.

C3-3 APPswe mice with the levels in C3-3 × PS1-A246E, C3-3 × PS1-dE9, APPswe/PS1dE9 line 85 and Q2-2 mice (Fig. 5A and Table 1). In the first series, all values were normalized to Aβ levels in the C3-3 mice. Graphing the relative levels of each peptide in these animals revealed that the addition of mutant PS1 increases the concentration of Aβ42 without causing a proportionate decrease in Aβ40. The case for this conclusion is stronger in the second series of mice described below, but even in the C3-3 series our measurements show that, compared with APPswe single transgenic mice, co-expression of PS1A246E caused a 50% increase, and PS1-dE9 a 150% increase, in the concentration of Aβ42 without consistently lowering the level of Aβ40. In mice co-expressing the PS1dE9 variant with APPswe, the levels of Aβ42 exceeded that of Aβ40 (Fig. 3), hence it is difficult to argue that the lack of change in Aβ40 levels might be due to a far greater abundance of Aβ40 relative to Aβ42.

Comparison of these values with the ages at which amyloid deposits first appear in each genotype suggests an immediate relationship (Fig. 5B). The age of onset in each cross directly correlates with the concentration of Aβ42 in the brain. This correlation extends beyond the C3-3 series. Line 85 mice, made by co-injecting APPswe and PS1dE9 vectors, were very similar to C3-3 × PS1-dE9 mice in both their peptide levels and in their age of amyloid onset (Fig. 5A and B). At the other end of this spectrum, Q2-2 single transgenic mice accumulate even less Aβ42 than C3-3 single transgenic mice, and show no sign of amyloid pathology at ages when deposits have already begun in C3-3 animals (Fig. 5A and B).

In the second ELISA experiment, we measured Aβ levels across the Q2-2 APPswe series (Q2-2; Q2-2 × PS1-A246E; and Q2-2 × PS1-dE9). The concentrations of Aβ values for each genotype were normalized to levels in the Q2-2 single transgenic animals. Again, we found that the addition of mutant PS1 specifically elevates Aβ42 levels without lowering Aβ40 levels (Fig. 5C and Table 1). Collectively these data demonstrate that when mutant PS1 is present, then there is a specific increase in Aβ42 without a proportionate decrease in Aβ40. These data also demonstrate that the concentration of Aβ42 is the driving force behind changes in the rate of amyloid deposition that occur in the double transgenic mice.

Transgenic mice expressing PS1-dE9 do not develop 'cotton wool' plaques

In FAD patients, the dE9 mutation is associated with pathology and motor symptoms atypical for AD. Neuropathological examination of several patients carrying this mutation have revealed large, loose, 'cotton wool' amyloid aggregates in the cortex, and a relative absence of compact dense core deposits (59–63). Such atypical pathology has not been found in all PS1-dE9 kindreds (62,64), and indeed, was not observed in mice expressing the dE9 transgene. Instead, APPswe/PS1-dE9 double transgenic animals displayed characteristic compact, dense-cored, deposits throughout the cortex and hippocampus which could be stained with Congo Red and were birefringent under polarized light (Fig. 6).

DISCUSSION

We have studied how the FAD variants of PS1 elevate Aβ levels and accelerate amyloid deposition to different extents in transgenic mice that co-express Mo/Hu APPswe. By comparing Aβ measurements in APPswe/PS1-dE9 double transgenic mice to animals expressing APPswe, alone or with the less pathogenic PS1-A246E mutation, we have gained insight into

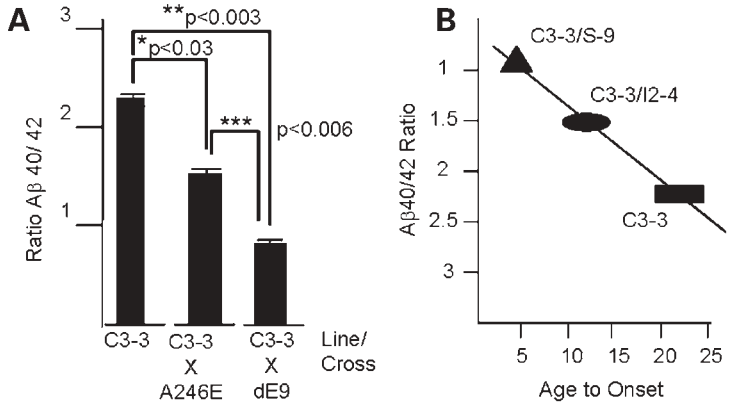

Figure 3. Co-expressing mutant PS1 shifts the ratio of Aβ40 : 42. (**A**) Quantitative immunoprecipitation and immunoblotting (see Methods) were used to measure Aβ40 : 42 ratios in the brains of mice co-expressing APPswe with PS1A246E or PS1dE9. In mice from line C3-3, the brains contains 2- to 3-fold more Aβ40 than Aβ42. As reported in a previous work (39), co-expression of PS1A246E halves the Aβ40 : Aβ42 ratio to ∼1.75. Here we show that expressing PS1dE9 in the C3-3 APPswe mice alters Aβ levels so dramatically that Aβ42 becomes the dominant species. (**B**) Regression analysis reveals a direct correlation between the age of amyloid onset and the ratio of Aβ40 : 42 in the C3-3 transgenic series. Statistical significance was determined by two-tailed Student's *t*-test.

the mechanisms by which mutations in PS1 cause early-onset AD. Our data show that FAD variants of PS1 selectively increase the levels of Aβ42 without affecting Aβ40 levels. Thus, co-expression of PS1 variants increases the amount of total Aβ derived from a constant level of APPswe protein, suggesting that mutant PS1, either directly or indirectly, makes more substrate available for γ-processing, and that this additional substrate is specifically cleaved at residue 42. We further demonstrate that small changes in the levels of Aβ42 can have considerable impact on the rate of amyloid deposition, highlighting the potential therapeutic benefit that might be gained by lowering Aβ42 levels, even partially, early in the clinical course of AD.

Amyloid onset is determined by the level of Aβ42

In previous studies, we (44,47) and others (42,43,48) have demonstrated that the co-expression of FAD-associated PS1 variants in APP transgenic mice shifts the ratio of Aβ40 : Aβ42, and that this shift correlates with a more rapid appearance of amyloid deposits. In contrast, the co-expression of wild-type human PS1 has no impact on the rate of amyloid formation (44). All previous studies have been two-point comparisons between one line of mice expressing mutant APP mice and mice expressing one FAD-PS1 variant. The present study is the first to analyze different combinations of APP and PS1 variants that show distinct courses of amyloid pathology. Our data demonstrate that the age at which amyloid deposits first appear correlates directly with the concentration of Aβ42 in the brain. As demonstrated in mice from line Q2-2, not all animals over-expressing APP, nor even those co-expressing PS1, will form amyloid deposits in their 2-year lifetime. While co-expression of PS1-A246E was able to dramatically accelerate the appearance of plaques in C3-3 APPswe transgenic mice, its effect was not strong enough to induce plaques by 20 months of age in the lower-expressing Q2-2 APPswe mice. Instead, plaques were only observed in mice from line Q2-2 when the highly pathogenic PS1-dE9 variant was introduced. Quantitative ELISA analysis in mice from each genotype revealed that both PS1 variants altered the concentration of Aβ42 in the brain: animals expressing either PS1 variant contained more Aβ42 than Q2-2 single transgenic mice. However, co-expression of PS1-dE9 led to substantially higher Aβ42 levels than did PS1-A246E, consistent with its ability to induce amyloid formation earlier than PS1-A246E.

Studies of Aβ40 and Aβ42 fibrilization *in vitro* have demonstrated that the formation of congophilic fibrils follows second-order kinetics, where there is a long lag phase (the nucleation and seeding phase) followed by an exponential phase of fibril formation until extinction of the substrate (12,13,65,66). Since the length of the lag phase is proportional to the concentration of Aβ peptides (12,13,65,66), we believe that the different rates of Aβ deposition observed in each genotype represent changes in the rate of nucleation and seeding of Aβ42 fibrils *in vivo.*

Congophilic neuritic amyloid pathology in Mo/Hu APPswe × PS1dE9 mice

Neuropathological studies of brains from FAD patients with the PS1-dE9 mutation have reported a number of cases that contain senile plaques atypical for AD. In these unusual cases, Aβ aggregates have been described as 'cotton wool' deposits because they lack compact dense cores and do not show birefringence when stained with Congo Red (59–63). However such atypical pathology has not been found in all PS1-dE9 kindreds (62,64). Indeed, mice carrying the PS1dE9 mutation do not recapitulate the cotton wool plaques of the dE9 FAD patients. Instead, all lines of APPswe/PS1dE9 mice examined in this study develop congophilic, neuritic, senile plaques (Fig. 6). Perhaps the extreme concentrations of Aβ needed to observe amyloid formation within the mouse lifespan artificially drive plaques into the compact form.

The second atypical feature of FAD caused by the PS1-dE9 mutation is the frequent appearance of spastic paraparesis (59,61,67). Affected patients exhibit abnormal gait with hyper-reflexive lower extremities. However, not all kindreds carrying PS1-dE9 show motor involvement (62). We have yet to observe

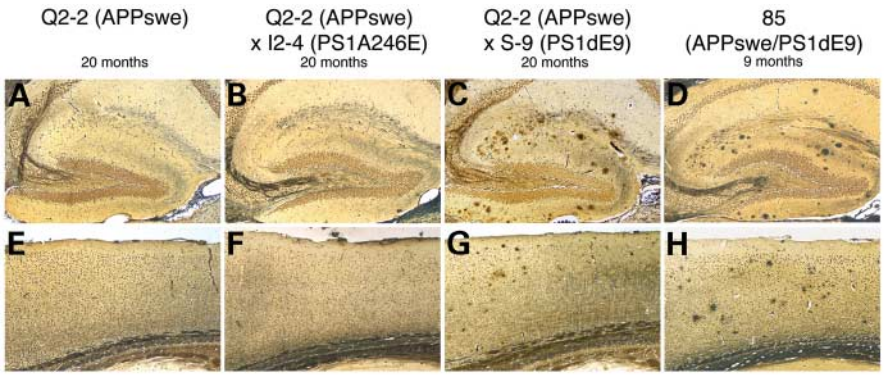

Figure 4. Co-expression of PS1-dE9 can induce plaque formation in a non-depositing line of APPswe transgenic mice. (**A** and **E**) Unlike previously published lines of APPswe transgenic mice, animals from line Q2-2 never develop amyloid deposits even at very late ages. Shown here are Hirano silver stained sections from the hippocampus (A) and cortex (E) of 20-month-old animals. (**B** and **F**) Co-expression of PS1-A246E is not sufficient too induce amyloidosis in mice from line Q2-2 before 20 months of age. (**C** and **G**) Co-expression of the more pathogenic PS1-dE9 leads to the formation of amyloid plaques in Q2-2 mice by 20 months of age. Diffuse and dense core deposits are found in both the hippocampus (C) and cortex (G) at this age. (**D** and **H**) Line 85 mice in which the APPswe and PS1-dE9 transgenes have been co-injected are shown for comparison. These animals express slightly higher levels of APPswe than line Q2-2 mice, leading to an earlier onset of pathology than Q2-2 × PS1dE9. Plaques are abundant in the hippocampus (D) and cortex (H) of line 85 mice by 9 months of age.

any evidence of diminished motor function in any line mice expressing PS1-dE9, either alone or in conjunction with APPswe (A. Savonenko *et al*., submitted). The incomplete penetrance of atypical pathology and motor dysfunction in the PS1-dE9 kindreds, and the lack of such features in the transgenic models, suggests that a modifier locus may influence the expression of these phenotypes in humans.

Mutant presenilins may recruit new pools of substrate to the γ-secretase pathway to elevate production of Aβ42

Studies of presenilin biology suggest that PS1 and PS2 compete for inclusion into a larger protein complex that contains nicastrin, Aph-1 and PEN-2 (18–27). This complex is required for active γ-secretase, which is responsible for proteolytic processing of APP to generate the C-termini of Aβ peptides (28,33). Studies with chemical inhibitors of γ-secretase have shown that the cleavage of APP at the 40 site and 42 sites are coordinately suppressed, suggesting a single activity is responsible for both cleavages (50,51,68–70). In this setting, the simplest explanation for the elevation of Aβ42 relative to Aβ40 in the presence of mutant PS1 was a simple shift in the enzyme specificity to favor cleavage at residue 42 with no net change in the amount of total Aβ. However, our results indicate that the expression of FAD PS1 variants specified increases in the steady-state levels of Aβ42 without altering Aβ 40 levels. Expression of mutant PS1 thus leads to a net increase in total Aβ. A similar finding was reported by Oyama and colleagues in their study of mice transgenic for PS2-N141I, which also show a specific increase in Aβ42 levels (46).

Experiments in cell cultures have shown that co-expression of FAD PS1 variants with APP alters the ratio of Aβ40 : 42 in the medium in favor of Aβ42 (39–41). In these cell culture experiments, it is assumed that the PS1 variants alter the production and secretion of Aβ42 rather than altering its clearance or catabolism. However, the cell culture paradigms cannot replicate the complex architecture and signaling patterns of neurons the brain. In hippocampal slice cultures, Kamenetz *et al.* (71) recently demonstrated that neuronal activity can influence the secretion of Aβ into the extracellular space. *In vivo*, such as with the animal models used for our studies, it is difficult to separate changes in the production of Aβ from changes in its catabolism. However, based on the cell culture studies of APP processing, we believe it likely that the increase in steady-state levels of Aβ42 measured in brain tissue from our mice reflects enhanced production of Aβ42, rather than changes in its stability or clearance. Studies demonstrating the absolute requirement of PS1 or PS2 function for an active γ-secretase (28,33) are consistent with this interpretation.

Recent reports indicate that PS1 is required for the translocation of APP from the plasma membrane into endosomes where the γ-secretase cleavage that produces extracellular Aβ is thought to occur (72), and that specific mutations in PS1 alter this movement (73–75). Moreover, others have demonstrated that cells deficient in PS1 show alterations in the subcellular trafficking of specific membrane proteins (36,37). However, studies in cultured cells have suggested that full-length APP is not the preferred substrate for γ-secretase. Instead, it appears that the direct substrates of γ-secretase are C-terminal fragments of APP generated by α- or β-secretase. These fragments, not the full-length protein, accumulate to high levels when γ-secretase is inhibited (28,30,31,33,49–52). Whether the effects we have detected are due to changes in APP trafficking is unclear. We note that an analysis of the levels of sAPP-β, the soluble ectodomain of APP generated by BACE1, failed to detect obvious alterations due to co-expression of mutant PS1 (Supplementaly Material, Fig. S1).

In light of foregoing data, we favor the notion that PS1-A246E and PS1-dE9, with differing efficiencies, place a greater amount of APP-CTF substrate in contact with a γ-secretase that preferentially cleaves at residue 42. This mechanism would explain the specific elevation in Aβ42 levels and the absence of change in Aβ40 levels. Moreover, this scenario could also explain how certain natural and experimental variants of PS1 differentially affect the cleavage of APP-CTFs and Notch, another important substrate of γ-secretase (32). We note that if the PS1/Nicastrin/PEN-2/Aph-1 protein complex were responsible for the delivery of substrates to γ-secretase but not their

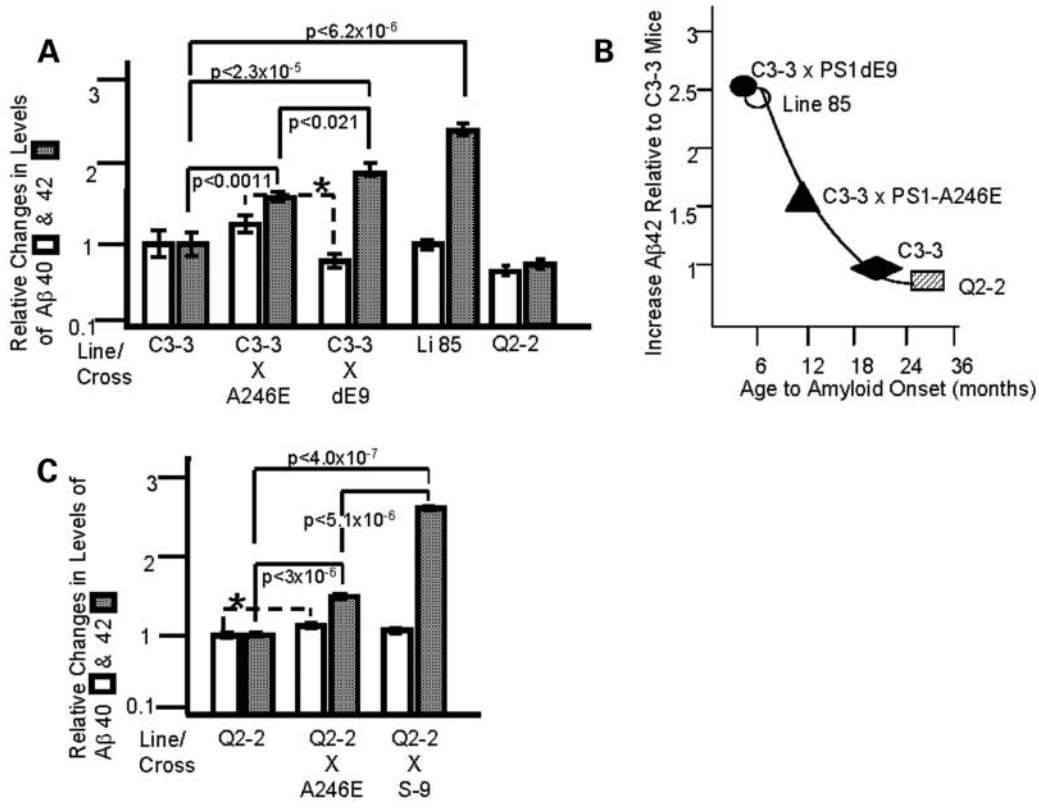

Figure 5. Mutant PS1 specifically elevates the levels of Aβ42 and proportionately decreases the age at which deposits first appear in APPswe transgenic mice. (**A**) The levels of Aβ40 and 42 were measured in the brains of mice from five distinct genotypes (noted below graph) by ELISA as described in Materials and Methods. Values for Aβ40 and 42 in each genotype were normalized to the levels in C3-3 single transgenic mice, so that the value of each peptide in the C3-3 mice is set to 1, and the values for Aβ40 and 42 in other genotypes are related to C3-3 mice (see Table 1). Statistical significance among genotypes was calculated pair-wise using a two-tailed Student's *t*-test (pairs noted by brackets on figure). The asterisk denotes a significant difference in Aβ40 levels between C3-3 × PS1-A246E and C3-3 × PS1-dE9 ($P < 0.0015$). There were no statistical differences in Aβ40 levels within the remaining C3-3 pairs. By contrast, levels of Aβ42 were significantly increased in mice co-expressing mutant PS1. (**B**) The relationship between brain concentration of Aβ42 and the age of amyloid onset for the genotypes analyzed in (A). As in (A), all Aβ42 values are normalized to the levels measured in C3-3 single transgenic animals. Co-expression of Hu PS1dE9 induces the greatest relative increase in Aβ42 and the largest decrease in age of amyloid onset. Note that the onset of amyloid lesions for line Q2-2 is estimated from the age at which plaques appear in Q2-2 × PS1dE9 animals, and would be difficult to observe in the normal mouse lifespan. (**C**) The levels of Aβ40 and 42 in the brains of Q2-2 APPswe mice crossed to PS1 mice were measured in a separate ELISA assay. The concentration of each peptide was normalized to the value measured in Q2-2 single transgenic mice (set to 1). As in the C3-3 series, the co-expression of PS1A246E and PS1dE9 in the Q2-2 mice significantly elevated the level of Aβ42 without decreasing that of Aβ40. The asterisk denotes a small but significant difference in Aβ40 found between Q2-2 × PS1-A246E and Q2-2. None of the remaining pairs showed significant differences in Aβ40.

proteolysis, inhibition of the PS1 complex, either genetically or pharmacologically, would diminish γ-secretase activity in a manner indistinguishable from inhibiting γ-secretase itself. Thus, we think it possible that one of the effects of mutant PS1 is to augment the amount of substrate presented to a 42-specific γ-secretase.

CONCLUSIONS

These studies have highlighted how small changes in the production of Aβ42 can modulate the rate of amyloid deposition. Within the limits imposed by the mouse lifespan, these small changes in Aβ42 levels can make the difference between the appearance and absence of amyloid pathology. We show here that this dichotomy is determined by a threshold concentration of Aβ42, and that once this minimum is surpassed further elevations in Aβ42 act to hasten the onset of amyloid aggregation. These findings suggest that even partial reductions of Aβ42 levels by pharmacological agents may substantially delay the onset of amyloid lesions in patients at risk for AD. Our study is also the first to demonstrate that the presence of mutant PS1 results in more Aβ42 by specifically increasing the concentration of this peptide without altering that of Aβ40. We suggest that mutant PS1 may act to recruit new pools of APP β-CTF substrate to a γ-secretase that favors cleavage at residue 42. Altering the subcellular trafficking of APP substrates could therefore be another therapeutic approach to diminish the concentration of Aβ42 the brains of patients with AD.

MATERIALS AND METHODS

Generation of transgenic mice

With the exception of line 85, all transgenic mice used in this study have been described and fully characterized in earlier

Table 1. Normalized fractions of brain Aβ extracted into DEA and formic acid

	Series 1									
	C3-3 APPswe ($n=9$)		C3-3 × N-5 APPswe × PS1A246E ($n=5$)		C3-3 × S-9 APPswe × PS1dE9 ($n=5$)		85 APPswe/PS1dE9 ($n=4$)		Q2-2 APPswe ($n=5$)	
	40	42	40	42	40	42	40	42	40	42
DEA	0.47 (0.131)	0.32 (0.071)	0.63 (0.089)	0.64 (0.072)	0.32 (0.057)	0.75 (0.118)	0.42 (0.058)	0.88 (0.104)	0.24 (0.009)	0.22 (0.012)
FA	0.53 (0.181)	0.68 (0.196)	0.61 (0.100)	0.93 (0.149)	0.48 (0.076)	1.32 (0.219)	0.60 (0.065)	1.56 (0.281)	0.45 (0.075)	0.60 (0.078)
Total	1.00 (0.302)	1.00 (0.261)	1.24 (0.168)	1.57 (0.192)	0.79 (0.132)	2.06 (0.330)	1.02 (0.120)	2.43 (0.377)	0.69 (0.069)	0.83 (0.078)

	Series 2					
	Q2-2 APPswe ($n=5$)		Q2-2 × I2-4 APPswe × PS1A246E ($n=5$)		Q2-2 × S-9 APPswe × PS1dE9 ($n=5$)	
	40	42	40	42	40	42
DEA	0.56 (0.063)	0.33 (0.023)	0.60 (0.047)	0.50 (0.030)	0.52 (0.029)	0.92 (0.110)
FA	0.44 (0.036)	0.67 (0.040)	0.52 (0.042)	0.97 (0.028)	0.55 (0.057)	1.69 (0.152)
Total	1.00 (0.035)	1.00 (0.058)	1.12 (0.057)	1.47 (0.035)	1.07 (0.080)	2.61 (0.234)

One hemisphere of each brain sample was sonicated in DEA, separated by centrifugation into soluble and insoluble fractions before the insoluble pellet was re-extracted with FA. The values in each table are normalized to the total amount of Aβ extracted from Line C3-3 (series 1) or Q2-2 (series 2) APPswe single transgenic mice. Values for Aβ40 and for Aβ42 have been normalized separately. The number of animals assayed is indicated for each genotype. Standard deviation for each measure is given in parentheses.

publications. All transgenes were expressed under control of the mouse prion protein promoter (MoPrP.Xho), which drives high protein expression in neurons and astrocytes of the CNS (53,57). Lines C3-3 and Q2-2 expressing mouse/human (Mo/Hu) chimeric APP695 (humanized Aβ domain) harboring the Swedish (K594M/N595L) mutation are described in Borchelt *et al.* (53). Line I2-4, which expresses human PS1-A246E, is described in Lee *et al.* (56) and Borchelt *et al.* (44). Lines S-9 and O-7, expressing human PS1-dE9, are described in Lee *et al.* (56). The Mo/HuAPPswe (line C3-3) and PS1A246E (line N-5) mice have been deposited in the Jackson Laboratories.

Line 85 is a companion to lines 7, 26, 56, and 57 that were described in Jankowsky *et al.* (55). All five lines were created by co-injection of chimeric mouse/human APPswe and human PS1-dE9 vectors controlled by independent mouse prion protein promoter elements. The two transgenes co-integrated and co-segregate as a single locus (55). Protein expression of transgenic APPswe in line 85 is comparable to that previously described for line 57 (55). Line 85 mice have been deposited in the Jackson Laboratories.

All animals used in this study were maintained in a hybrid background by back-crossing to C3HeJ × C57BL/6J F_1 mice obtained from Jackson Laboratories (Bar Harbor, ME, USA). Offspring were genotyped for the presence of the transgene by PCR amplification of genomic DNA extracted from 1 cm tail clippings, as described in Jankowsky *et al.* (55). Reactions contained three primers, one antisense primer matching sequence within the vector that is also present in mouse genomic PrP (5′-GTG GAT ACC CCC TCC CCC AGC CTA GAC C), one sense primer specific for the transgene cDNA (PS1: 5′-CAG GTG GTG GAG CAA GAT G; APP: 5′-CCG AGA TCT CTG AAG TGA AGA TGG ATG), and a second sense primer specific for the genomic PrP coding region (which was removed from the MoPrP vector); (5′-CCT CTT TGT GAC TAT GTG GAC TGA TGT CGG). All reactions give a 750 bp product from the endogenous PrP gene as a control for DNA integrity and successful amplification; transgene-positive samples have an additional band at 400 bp (APP) or 1.3 kb (PS1).

Animals were housed in microisolator cages with unlimited access to food and water. All procedures involving animals were approved by the JHU Institutional Animal Care and Use Committee.

Aβ peptide analysis by quantitative immunoblot

Quantitation of Aβ levels in transgenic mouse brain tissue was performed as described in Lesuisse *et al.* (57). Briefly, hemibrain samples from line C3-3 mice were homogenized with a Dounce tissue grinder in 24 vols of PBS containing 1% CHAPS, 1 mM PMSF, 5 μg/ml leupeptin, 30 μg/ml aprotinin, and 1 μM pepstatin. Homogenates were mixed for 30 min at 4°C, and then centrifuged for 1 h at 100 000*g*. Supernatants were immunoprecipitated with monoclonal antibody 26D6 (specific for Aβ1-12), and recovered peptides were separated by bicine/urea SDS–PAGE. Proteins were transferred to PVDF membrane and blotted with 26D6 conjugated to horseradish peroxidase. Antibody binding was visualized with ECL reagent exposed to film, and quantified using scanning laser densitometry to compare band densities for each sample to synthetic Aβ standards run in parallel. Statistics were performed by one-way ANOVA with least-square difference (LSD) post-test using the Statistica analysis program (StatSoft, Tulsa, OK, USA).

Aβ peptide quantitation by ELISA

Frozen mouse hemi-brains ($n=4$–5 per genotype) were extracted by sonication in 0.2% diethylamine (DEA)/50 mM NaCl to a concentration of 100 mg/ml. After centrifugation at 100 000*g* for 1 h at 4°C, the supernatant was removed and saved as the DEA extract. The pellet was then sonicated in 70% formic acid (FA) diluted in water, using a volume equal to the original

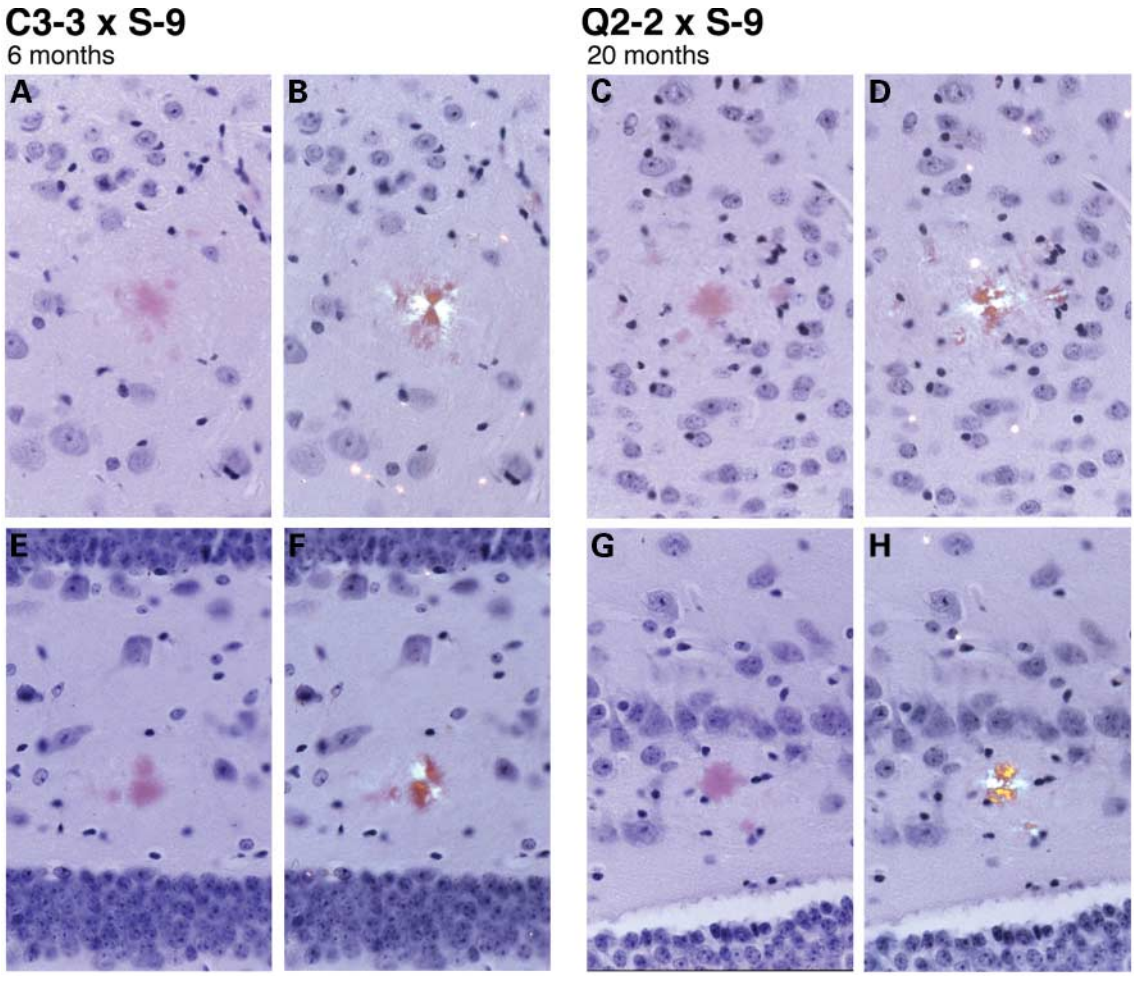

Figure 6. Congophilic amyloid deposits are found in mice co-expressing PS1-dE9 and APPswe. (**A–H**) Mice expressing the dE9 mutation of PS1 in conjunction with Mo/Hu APPswe develop typical diffuse and compact, birefringent, deposits. This panel shows Congo Red-stained plaques under bright-field (A, C, E and G) and under polarized light (B, D, F and H). The plaques appear qualitatively identical in mice from both high-expressing, early onset C3-3 and low-expressing, late-onset Q2-2 lines. Shown are sections from 6-month old C3-3 × PS1-dE9 mice (A, B, E and F) and 20-month-old Q2-2 × PS1-dE9 mice (C, D, G and H). Congophilic deposits are found both in the cortex (A–D) and in the hippocampus (E–H).

volume of DEA. After centrifugation at 100 000*g* for 1 h at 4°C, the supernatant was removed and saved as the FA extract.

Brain extracts were measured by sandwich ELISA as described previously (11,58,76). The DEA extracts were neutralized by adding 1/10 vol of 0.5 M Tris–HCl, pH 6.8. After vortexing briefly, neutralized samples were prepared for ELISA by 1 : 10 dilution in EC buffer (0.02 M phosphate buffer, pH 7, 0.4 M NaCl, 2 mM EDTA, 0.4% Block Ace (Dainipponseiyaku, Suita, Osaka, Japan), 0.2% bovine serum albumin, 0.05% CHAPS, and 0.05% sodium azide. The standard curve used to calculate Aβ concentration of DEA extracts was also performed in EC buffer. The FA extracts were neutralized and prepared for ELISA by diluting 1 : 20 in 1 M Tris–phosphate buffer (TPB), pH 11. The standard curve for FA extracts was performed in the same mixture of FA and TPB. All samples were assayed with a human-Aβ-specific ELISA system, which uses the BAN50 monoclonal antibody (mAb; epitope Aβ1-16) for capture and the BA27 and BC05 mAbs for detection of Aβ40 and Aβ42, respectively. Final Aβ concentrations were expressed as picomoles per gram tissue, calculated from the original brain weight measurement prior to homogenization.

Statistics were performed by one-way ANOVA with (LSD) post-test using the Statistica analysis program (StatSoft, Tulsa, OK, USA).

Histology

Mice were euthanized by ether inhalation and the brain removed for immersion in 4% paraformaldehyde/1 × buffered saline (PBS). After fixation for 48 h at 4°C, brains were transferred to PBS, dehydrated in an alcohol series, treated with cedarwood oil and methylsalicylate, and embedded in paraffin for sectioning.

Hirano silver stain. Silver impregnation histology was performed on 10 μm paraffin-embedded sections by Hirano's modification of the Bielschowsky method (77,78). Briefly, sections were deparaffinized through xylene and alcohols into tap water before being placed into fresh 20% silver nitrate solution for

20 min. After washing thoroughly with distilled water, slides were immersed in 20% silver nitrate solution titrated with fresh ammonium hydroxide. After 20 min, slides were washed with ammonia water before being individually developed with 100 µl of developer (20 ml of 37% formaldehyde, 100 ml distilled water, 50 µl concentrated nitric acid and 0.5 g citric acid) added to 50 ml of titrated silver nitrate solution. Slides were then rinsed in tap water, fixed in 5% sodium thiosulfate, and dehydrated through alcohols and xylene.

Congo Red stain. Congo Red staining was performed according to standard techniques. Deparaffinized slides with 10 µm brain sections were counterstained in hematoxylin, rinsed well, then immersed in congo red solution 20 g sodium chloride in 100 ml distilled water mixed with 5 g Congo Red (Sigma, St Louis, MO, USA) dissolved in 400 ml 95% ethanol for 30 min. Without rinsing, slides were moved into aniline blue (7.5 g aniline blue, 5 ml glacial acetic acid, and 250 ml distilled water), then dehydrated in ethanol and xylene.

Western blotting

Western blotting to assess transgenic APP expression in the Q2-2, 85 and C3-3 lines was performed as described in Jankowsky *et al.* (55). Briefly, 5 or 50 µg of brain homogenate (when probed by 22C11 or 6E10 and antiSEVNL, respectively) were loaded per lane onto a 10% Tris–glycine SDS–PAGE gel (Invitrogen, Carlsbad, CA, USA) and electrophoresed for several hours in 1 × TG–SDS buffer (Amresco, Solon, OH, USA). Proteins were transferred overnight to 0.45 µm Optitran nitrocellulose (Schleicher and Schuell, Keene, NH, USA) in 1 × TG buffer (Amresco). Blots were blocked in PBS containing 5% non-fat dry milk powder, and incubated for 3 h at room temperature with either antibody 22C11 (kind gift of Drs Konrad Beyreuther and Andreas Weidemann) diluted 1 : 2000 in blocking solution, antibody 6E10 Signet Laboratories (Dedham, MA, USA) diluted 1 : 2500 in blocking solution, or α-SEVNL (79) diluted 1 : 2000 in blocking solution. The blots were washed several times with PBS containing 0.1% Tween-20, and then incubated either in peroxidase-conjugated protein A (Sigma, St Louis, MO, USA) diluted 1 : 2000 in blocking solution or (for 6E10) in a mixture of peroxidase-protein A diluted 1 : 1000 and rabbit anti-mouse IgG (Chemicon, Temecula, CA, USA) diluted 1 : 2000 in blocking solution. After washing several times in PBS with 0.1% Tween-20, blots were developed with enhanced chemiluminescence reagent (New England Nuclear, Boston, MA, USA) and exposed to film.

The levels of PS1 transgene products in the mice used here have been previously described (39,44,56). The steady-state levels of human PS1 protein in the various mice used here accumulate to similar levels (44,56).

SUPPLEMENTARY MATERIAL

Supplementary Material is available at HMG Online.

ACKNOWLEDGEMENTS

We thank Debbie Swing for assistance with the production of transgenic mice, and David Fromholt and Alvin George for help with mouse genotyping. Data on crosses of Mo/Hu APPswe line C3-3 to PS1-dE9 line O-7 were kindly provided by Drs. Shadid Zaman, Flavio Kamenetz, and Roberto Malinow (Cold Spring Harbor Laboratory, Cold Spring Harbor, NY, USA). We are grateful to Drs Konrad Beyreuther and Andreas Weidemann for sharing the 22C11 antibody, and to Dr Robert Siman (University of Pennsylvania Medical School) for sharing the anti-SEVNL antibody. This work was funded by grants from the National Institute of Aging (D.R.B.; NIA 1 P50 AG 14248 and NIA 1 P01 AG-98-003), the National Cancer Institute (N.A.J. and N.G.C.), and the Alzheimer's Association (D.R.B.). J.L.J. was supported by a training grant (NIH 1 T32 NS 07435), and by funding from the John Douglas French Alzheimer's Foundation and the American Health Assistance Foundation.

REFERENCES

1. Jankowsky, J.L., Savonenko, A., Schilling, G., Wang, J., Xu, G. and Borchelt, D.R. (2002) Transgenic mouse models of neurodegenerative disease: opportunities for therapeutic development. *Curr. Neurol. Neurosci. Rep.*, **2**, 457–464.
2. Glenner, G.G. and Wong, C.W. (1984) Alzheimer's disease and Down's syndrome: sharing of a unique cerebrovascular amyloid fibril protein. *Biochem. Biophys. Res. Commun.*, **122**, 1131–1135.
3. Masters, C.L., Simms, G., Weinman, N.A., Multhaup, G., McDonald, B.L. and Beyreuther, K. (1985) Amyloid plaque core protein in Alzheimer disease and Down syndrome. *Proc. Natl Acad. Sci. USA*, **82**, 4245–4249.
4. Roher, A., Wolfe, D., Palutke, M. and KuKurga, D. (1986) Purification, ultrastructure, and chemical analysis of Alzheimer disease amyloid plaque core protein. *Proc. Natl Acad. Sci. USA*, **83**, 2662–2666.
5. Shoji, M., Golde, T.E., Ghiso, J., Cheung, T.T., Estus, S., Shaffer, L.M., Cai, X.-D., McKay, D.M., Tintner, R., Frangione, B. and Younkin, S.G. (1992) Production of the Alzheimer amyloid β protein by normal proteolytic processing. *Science*, **258**, 126–129.
6. Haass, C., Schlossmacher, M.G., Hung, A.Y., Vigo-Pelfrey, C., Mellon, A., Ostaszewski, B.L., Lieberburg, I., Koo, E.H., Schenk, D., Teplow, D.B. and Selkoe, D.J. (1992) Amyloid β-peptide is produced by cultured cells during normal metabolism. *Nature*, **359**, 322–325.
7. Roher, A.E., Lowenson, J.D., Clarke, S., Woods, A.S., Cotter, R.J., Gowing, E. and Ball, M.J. (1993) beta-Amyloid-(1–42) is a major component of cerebrovascular amyloid deposits: implications for the pathology of Alzheimer disease. *Proc. Natl Acad. Sci. USA*, **90**, 10836–10840.
8. Citron, M., Oltersdorf, T., Haass, C., McConlogue, L., Hung, A.Y., Seubert, P., Vigo-Pelfrey, C., Lieberburg, I. and Selkoe, D.J. (1992) Mutation of the β-amyloid precursor protein in familial Alzheimer's disease increases β-protein production. *Nature*, **360**, 672–674.
9. Cai, X.-D., Golde, T.E. and Younkin, S.G. (1993) Release of excess amyloid β protein from a mutant amyloid β protein precursor. *Science*, **259**, 514–516.
10. Haass, C., Hung, A.Y., Selkoe, D.J. and Teplow, D.B. (1994) Mutations associated with a locus for familial Alzheimer's disease result in alternative processing of amyloid β-protein precursor. *J. Biol. Chem.*, **269**, 17741–17748.
11. Suzuki, N., Cheung, T.T., Cai, X.-D., Odaka, A., Otvos, L., Jr., Eckman, C., Golde, T.E. and Younkin, S.G. (1994) An increased percentage of long amyloid β protein secreted by familial amyloid β protein precursor (βAPP_{717}) mutants. *Science*, **264**, 1336–1340.
12. Burdick, D., Soreghan, B., Kwon, M., Kosmoski, J., Knauer, M., Henschen, A., Yates, J., Cotman, C. and Glabe, C. (1992) Assembly and aggregation properties of synthetic Alzheimer's A4/β amyloid peptide analogs. *J. Biol. Chem.*, **267**, 546–554.
13. Jarrett, J.T., Lansbury, P.T., Jr. (1993) Seeding 'one-dimensional crystallization' of amyloid: a pathogenic mechanism in Alzheimer's disease and scrapie? *Cell*, **73**, 1055–1058.

14. Iwatsubo, T., Odaka, A., Suzuki, N., Mizusawa, H., Nukina, N. and Ihara, Y. (1994) Visualization of Aβ42(43)-positive and Aβ40-positive senile plaques with end-specific Aβ-monoclonal antibodies: evidence that an initially deposited Aβ species is Aβ1-42(43). *Neuron*, **13**, 45–53.
15. Rogaev, E.I., Sherrington, R., Rogaeva, E.A., Levesque, G., Ikeda, M., Liang, Y., Chi, H., Lin, C., Holman, K., Tsuda, T. *et al.* (1995) Familial Alzheimer's disease in kindreds with missense mutations in a gene on chromosome 1 related to the Alzheimer's disease type 3 gene. *Nature*, **376**, 775–778.
16. Sherrington, R., Rogaev, E.I., Liang, Y., Rogaeva, E.A., Levesque, G., Ikeda, M., Chi, H., Lin, C., Li, G. *et al.* (1995) Cloning of a gene bearing missense mutations in early-onset familial Alzheimer's disease. *Nature*, **375**, 754–760.
17. Sherrington, R., Froelich, S., Sorbi, S., Campion, D., Chi, H., Rogaeva, E.A., Levesque, G., Rogaev, E.I., Lin, C. *et al.* (1996) Alzheimer's disease associated with mutations in presenilin 2 is rare and variably penetrant. *Hum. Mol. Genet.*, **5**, 985–988.
18. Thinakaran, G., Harris, C.L., Ratovitski, T., Davenport, F., Slunt, H.H., Price, D.L., Borchelt, D.R. and Sisodia, S.S. (1997) Evidence that levels of presenilins (PS1 and PS2) are coordinately regulated by competition for limiting cellular factors. *J. Biol. Chem.*, **272**, 28415–28422.
19. Yu, G., Nishimura, M., Arawaka, S., Levitan, D., Zhang, L., Tandon, A., Song, Y.Q., Rogaeva, E., Chen, F., Kawaral, T. *et al.* (2000) Nicastrin modulates presenilin-mediated *notch/glp-1* signal transduction and beta-APP processing. *Nature*, **407**, 48–54.
20. Chung, H.M. and Struhl, G. (2001) Nicastrin is required for Presenilin-mediated transmembrane cleavage in *Drosophila*. *Nat. Cell Biol.*, **3**, 1129–1132.
21. Edbauer, D., Winkler, E., Haass, C. and Steiner, H. (2002) Presenilin and nicastrin regulate each other and determine amyloid beta-peptide production via complex formation. *Proc. Natl Acad. Sci. USA*, **99**, 8666–8671.
22. Hu, Y., Ye, Y. and Fortini, M.E. (2002) Nicastrin is required for γ-secretase cleavage of the *Drosophila* notch receptor. *Dev. Cell*, **2**, 69–78.
23. Lee, S.F., Shah, S., Li, H., Yu, C., Han, W. and Yu, G. (2002) Mammalian APH-1 interacts with presenilin and nicastrin, and is required for intramembrane proteolysis of APP and Notch. *J. Biol. Chem.*, **277**, 45013–45019.
24. Lopez-Schier, H. and St Johnston, D. (2002) Drosophila nicastrin is essential for the intramembranous cleavage of notch. *Dev. Cell*, **2**, 79–89.
25. Steiner, H., Winkler, E., Edbauer, D., Prokop, S., Basset, G., Yamasaki, A., Kostka, M. and Haass, C. (2002) PEN-2 is an integral component of the gamma-secretase complex required for coordinated expression of presenilin and nicastrin. *J. Biol. Chem.*, **277**, 39062–39065.
26. Takasugi, N., Tomita, T., Hayashi, I., Tsuruoka, M., Niimura, M., Takahashi, Y., Thinakaran, G. and Iwatsubo, T. (2003) The role of presenilin cofactors in the gamma-secretase complex. *Nature*, **422**, 438–441.
27. Luo, W.J., Wang, H., Li, H., Kim, B.S., Shah, S., Lee, H.J., Thinakaran, G., Kim, T.W., Yu, G. and Xu, H. (2003) PEN-2 and APH-1 coordinately regulate proteolytic processing of presenilin 1. *J. Biol. Chem.*, **278**, 7850–7854.
28. De Strooper, B., Saftig, P., Craessaerts, K., Vanderstichele, H., Guhde, G., Annaert, W., Von Figura, K. and Van Leuven, F. (1998) Deficiency of presenilin-1 inhibits the normal cleavage of amyloid precursor protein. *Nature*, **391**, 387–390.
29. Ray, W.J., Yao, M., Mumm, J., Schroeter, E.H., Saftig, P., Wolfe, M., Selkoe, D.J., Kopan, R. and Goate, A.M. (1999) Cell surface presenilin-1 participates in the gamma-secretase-like proteolysis of Notch. *J. Biol. Chem.*, **274**, 36801–36807.
30. De Strooper, B., Annaert, W., Cupers, P., Saftig, P., Craessaerts, K., Mumm, J.S., Schroeter, E.H., Schrijvers, V., Wolfe, M.S., Ray, W.J., Goate, A. and Kopan, R. (1999) A presenilin-1-dependent-secretase-like protease mediates release of notch intracellular domain. *Nature*, **398**, 518–522.
31. Wolfe, M.S., Xia, W., Ostazewski, B.L., Diehl, T.S., Kimberly, W.T. and Selkoe, D.J. (1999) Two transmembrane aspartates in presenilin-1 required for presenilin endoproteolysis and gamma-secretase activity. *Nature*, **398**, 513–517.
32. Capell, A., Steiner, H., Romig, H., Keck, S., Baader, M., Grim, M.G., Baumeister, R. and Haass, C. (2000) Presenilin-1 differentially facilitates endoproteolysis of the β-amyloid precursor protein and Notch. *Nat. Cell Biol.*, **2**, 205–211.
33. Herreman, A., Serneels, L., Annaert, W., Collen, D., Schoonjans, L. and De Strooper, B. (2000) Total inactivation of gamma-secretase activity in presenilin-deficient embryonic stem cells. *Nat. Cell Biol.*, **2**, 461–462.
34. Zhang, Z., Nadeau, P., Song, W., Donoviel, D., Yuan, M., Bernstein, A. and Yankner, B.A. (2000) Presenilins are required for gamma-secretase cleavage of beta-APP and transmembrane cleavage of Notch-1. *Nat. Cell Biol.*, **2**, 463–465.
35. Sastre, M., Steiner, H., Fuchs, K., Capell, A., Multhaup, G., Condron, M., Teplow, D. and Haass, C. (2001) Presenilin-dependent γ-secretase processing of β-amyloid precursor protein at a site corresponding to the S3 cleavage of notch. *Sci. Rep.*, **2**, 835–841.
36. Naruse, S., Thinakaran, G., Luo, J.J., Kusiak, J.W., Tomita, T., Iwatsubo, T., Qian, X., Ginty, D.D., Price, D.L., Borchelt, D.R., Wong, P.C. and Sisodia, S.S. (1998) Effects of PS1 deficiency on membrane protein trafficking in neurons. *Neuron*, **21**, 1213–1221.
37. Cai, D., Leem, J.Y., Greenfield, J.P., Wang, P., Kim, B.S., Wang, R., Lopes, K.O., Kim, S.H., Zheng, H., Greengard, P., Sisodia, S.S., Thinakaran, G. and Xu, H. (2003) Presenilin-1 regulates intracellular trafficking and cell surface delivery of beta-amyloid precursor protein. *J. Biol. Chem.*, **278**, 3446–3454.
38. Scheuner, D., Eckman, C., Jensen, M., Song, X., Citron, M., Suzuki, N., Bird, T.D., Hardy, J., Hutton, M., Kukull, W. *et al.* (1996) Secreted amyloid β-protein similar to that in the senile plaques of Alzheimer's disease is increased *in vivo* by the presenilin 1 and 2 and *APP* mutations linked to familial Alzheimer's disease. *Nat. Med.*, **2**, 864–870.
39. Borchelt, D.R., Thinakaran, G., Eckman, C.B., Lee, M.K., Davenport, F., Ratovitsky, T., Prada, C.-M., Kim, G., Seekins, S., Yager, D. *et al.* (1996) Familial Alzheimer's disease-linked presenilin 1 variants elevate Aβ1-42/1-40 ratio *in vitro* and *in vivo*. *Neuron*, **17**, 1005–1013.
40. Citron, M., Westaway, D., Xia, W., Carlson, G., Diehl, T., Levesque, G., Johnson-Wood, K., Lee, M., Seubert, P., Davis, A. *et al.* (1997) Mutant presenilins of Alzheimer's disease increase production of 42-residue amyloid β-protein in both transfected cells and transgenic mice. *Nat. Med.*, **3**, 67–72.
41. Tomita, T., Maruyama, K., Saido, T.C., Kume, H., Shinozaki, K., Tokuhiro, S., Capell, A., Walter, J., Grunberg, J., Haass, C., Iwatsubo, T. and Obata, K. (1997) The presenilin 2 mutation (N141I) linked to familial Alzheimer disease (Volga German families) increases the secretion of amyloid β protein ending at the 42nd (or 43rd) residue. *Proc. Natl Acad. Sci. USA*, **94**, 2025–2030.
42. Lamb, B.T., Bardel, K.A., Kulnane, L.S., Anderson, J.J., Holtz, G., Wagner, S.L., Sisodia, S.S. and Hoeger, E.J. (1999) Amyloid production and deposition in mutant amyloid precursor protein and presenilin-1 yeast artificial chromosome transgenic mice. *Nat. Neurosci.*, **2**, 695–697.
43. Dewachter, I., van Dorple, J., Spittaels, K., Tesseur, I., Van den Haute, C., Moechars, D. and Van Leuven, F. (2000) Modeling Alzheimer's disease in transgenic mice: effect of age and presenilin 1 on amyloid biochemistry and pathology in APP/London mice. *Exp. Gerontol.*, **35**, 831–841.
44. Borchelt, D.R., Lee, M.K., Gonzales, V., Slunt, H.S., Ratovitski, T., Jenkins, N.A., Copeland, N.G., Price, D.L. and Sisodia, S.S. (2001) Accumulation of proteolytic fragments of mutant presenilin 1 and accelerated amyloid deposition are co-regulated in transgenic mice. *Neurobiol. Aging*, **23**, 171–177.
45. Duff, K. (1997) Alzheimer transgenic mouse models come of age. *Trends Neurosci.*, **20**, 279–280.
46. Oyama, F., Sawamura, N., Kobayashi, K., Morishima-Kawashima, M., Kuramochi, T., Ito, M., Tomita, T., Maruyama, K., Saido, T.C., Iwatsubo, T. *et al.* (1998) Mutant presenilin 2 transgenic mouse: effect on an age-dependent increase of amyloid beta-protein 42 in the brain. *J. Neurochem.*, **71**, 313–322.
47. Borchelt, D.R., Ratovitski, T., Van Lare, J., Lee, M.K., Gonzales, V.B., Jenkins, N.A., Copeland, N.G., Price, D.L. and Sisodia, S.S. (1997) Accelerated amyloid deposition in the brains of transgenic mice co-expressing mutant presenilin 1 and amyloid precursor proteins. *Neuron*, **19**, 939–945.
48. Holcomb, L., Gordon, M.N., McGowan, E., Yu, X., Benkovic, S., Jantzen, P., Wright, K., Saad, I., Mueller, R., Morgan, D. *et al.* (1998) Accelerated Alzheimer-type phenotype in transgenic mice carrying both mutant amyloid precursor protein and presenilin 1 transgenes. *Nat. Med.*, **4**, 97–100.
49. Chen, F., Yang, D.S., Petanceska, S., Yang, A., Tandon, A., Yu, G., Rozmahel, R., Ghiso, J., Nishimura, M., Zhang, D.M. *et al.* (2000) Carboxyl-terminal fragments of alzheimer beta-amyloid precursor protein accumulate in restricted and unpredicted intracellular compartments in presenilin 1-deficient cells. *J. Biol. Chem.*, **275**, 36794–36802.

50. Esler, W.P., Taylor Kimberly, W., Ostaszewski, B.L., Diehl, T.S., Moore, C.L., Tsai, J.Y., Rahmati, T., Xia, W., Selkoe, D.J. and Wolfe, M.S. (2000) Transition-state analogue inhibitors of γ-secretase bind directly to presenilin-1. *Nat. Cell Biol.*, **2**, 1–7.
51. Xia, W., Ostaszewski, B.L., Kimberly, W.T., Rahmati, T., Moore, C.L., Wolfe, M.S. and Selkoe, D.J. (2000) FAD mutations in presenilin-1 or amyloid precursor protein decrease the efficacy of a gamma-secretase inhibitor: evidence for direct involvement of PS1 in the gamma-secretase cleavage complex. *Neurobiol. Dis.*, **7**, 673–681.
52. Xia, W., Zhang, J., Ostaszewski, B.L., Kimberly, W.T., Seubert, P., Koo, E.H., Shen, J. and Selkoe, D.J. (1998) Presenilin 1 regulates the processing of beta-amyloid precursor protein C-terminal fragments and the generation of amyloid beta-protein in endoplasmic reticulum and Golgi. *Biochemistry*, **37**, 16465–16471.
53. Borchelt, D.R., Davis, J., Fischer, M., Lee, M.K., Slunt, H.H., Ratovitsky, T., Regard, J., Copeland, N.G., Jenkins, N.A., Sisodia, S.S. and Price, D.L. (1996) A vector for expressing foreign genes in the brains and hearts of transgenic mice. *Genet. Anal. (Biomed. Eng.)*, **13**, 159–163.
54. Perez-Tur, J., Froelich, S., Prihar, G., Crook, R., Baker, M., Duff, K., Wragg, M., Busfield, F., Lendon, C., Clark, R.F. *et al.* (1995) A mutation in Alzheimer's disease destroying a splice acceptor site in the presenilin-1 gene. *Neuroreport*, **7**, 297–301.
55. Jankowsky, J.L., Slunt, H.H., Ratovitski, T., Jenkins, N.A., Copeland, N.G. and Borchelt, D.R. (2001) Co-expression of multiple transgenes in mouse CNS: a comparison of strategies. *Biomol. Eng.*, **17**, 157–165.
56. Lee, M.K., Borchelt, D.R., Kim, G., Thinakaran, G., Slunt, H.H., Ratovitski, T., Martin, L.J., Kittur, A., Gandy, S., Levey, A.I., Jenkins, N., Copeland, N., Price, D.L. and Sisodia, S.S. (1997) Hyperaccumulation of FAD-linked presenilin 1 variants *in vivo*. *Nat. Med.*, **3**, 756–760.
57. Lesuisse, C., Xu, G., Anderson, J., Wong, M., Jankowsky, J., Holtz, G., Gonzalez, V., Wong, P.C.Y., Price, D.L., Tang, F., Wagner, S. and Borchelt, D.R. (2001) Hyper-expression of human apolipoprotein E4 in astroglia and neurons does not enhance amyloid deposition in transgenic mice. *Hum. Mol. Genet.*, **10**, 2525–2537.
58. Kawarabayashi, T., Younkin, L.H., Saido, T.C., Shoji, M., Ashe, K.H. and Younkin, S.G. (2001) Age-dependent changes in brain, CSF, and plasma amyloid (beta) protein in the Tg2576 transgenic mouse model of Alzheimer's disease. *J. Neurosci.*, **21**, 372–381.
59. Smith, M.J., Kwok, J.B., McLean, C.A., Kril, J.J., Broe, G.A., Nicholson, G.A., Cappai, R., Hallupp, M., Cotton, R.G., Masters, C.L., Schofield, P.R. and Brooks, W.S. (2001) Variable phenotype of Alzheimer's disease with spastic paraparesis. *Ann. Neurol.*, **49**, 125–129.
60. Steiner, H., Revesz, T., Neumann, M., Romig, H., Grim, M.G., Pesold, B., Kretzschmar, H.A., Hardy, J., Holton, J.L., Baumeister, R., Houlden, H. and Haass, C. (2001) A pathogenic presenilin-1 deletion causes aberrant Abeta 42 production in the absence of congophilic amyloid plaques. *J. Biol. Chem.*, **276**, 7233–7239.
61. Crook, R., Chen, L.S., Bende, S.M. and LaFerla, F.M. (1998) A variant of Alzheimer's disease wtih spastic paraparaesis and unusual plaques due to deletion of exon 9 of presenilin 1. *Nat. Med.*, **4**, 1–4.
62. Hiltunen, M., Helisalmi, S., Mannermaa, A., Alafuzoff, I., Koivisto, A.M., Lehtovirta, M., Pirskanen, M., Sulkava, R., Verkkoniemi, A. and Soininen, H. (2000) Identification of a novel 4.6-kb genomic deletion in presenilin-1 gene which results in exclusion of exon 9 in a Finnish early onset Alzheimer's disease family: an Alu core sequence-stimulated recombination? *Eur. J. Hum. Genet.*, **8**, 259–266.
63. Mann, D.M., Takeuchi, A., Sato, S., Cairns, N.J., Lantos, P.L., Rossor, M.N., Haltia, M., Kalimo, H. and Iwatsubo, T. (2001) Cases of Alzheimer's disease due to deletion of exon 9 of the presenilin-1 gene show an unusual but characteristic beta-amyloid pathology known as 'cotton wool' plaques. *Neuropathol. Appl. Neurobiol.*, **27**, 189–196.
64. Ishii, K., Ii, K., Hasegawa, T., Shoji, S., Doi, A. and Mori, H. (1997) Increased Aβ 42(43)-plaque depostion in early-onset familial Alzheimer's disease brains with the deletion of exon 9 and the missense point mutation (H163R) in the PS-1 gene. *Neurosci. Lett.*, **228**, 17–20.
65. Jarrett, J.T., Berger, E.P. and Lansbury, P.T. Jr (1993) The carboxy terminus of the β amyloid protein is critical for the seeding of amyloid formation: implications for the pathogenesis of Alzheimer's disease. *Biochemistry*, **32**, 4693–4697.
66. Jarrett, J.T. and Lansbury, P.T., Jr (1992) Amyloid fibril formation requires a chemically discriminating nucleation event: studies of an amyloidogenic sequence from the bacterial protein OsmB. *Biochemistry*, **31**, 12345–12352.
67. Houlden, H., Baker, M., McGowan, E., Lewis, P., Hutton, M., Crook, R., Wood, N.W., Kumar-Singh, S., Geddes, J., Swash, M. *et al.* (2000) Variant Alzheimer's disease with spastic paraparesis and cotton wool plaques is caused by PS-1 mutations that lead to exceptionally high amyloid-beta concentrations. *Ann. Neurol.*, **48**, 806–808.
68. Wolfe, M.S., Citron, M., Diehl, T.S., Xia, W., Donkor, I.O. and Selkoe, D.J. (2000) A substrate-based difluoro ketone selectively inhibits Alzheimer's -secretase activity. *J. Med. Chem.*, **41**, 6–9.
69. Li, Y.M., Xu, M., Lai, M.T., Huang, Q., Castro, J.L., DiMuzio-Mower, J., Harrison, T., Lellis, C., Nadin, A., Neduvelil, J.G. *et al.* (2000) Photoactivated γ-secretase inhibitors directed to the active site convalently label presenilin 1. *Nature*, **405**, 689–693.
70. Seiffert, D., Bradley, J.D., Rominger, C.M., Rominger, D.H., Yang, F., Meredith, J.E. Jr Wang, Q., Roach, A.H., Thompson, L.A., Spitz, S.M. et al. (2000) Presenilin-1 and -2 are molecular targets for gamma-secretase inhibitors. *J. Biol. Chem.*, **275**, 34086–34091.
71. Kamenetz, F., Tomita, T., Hsieh, H., Seabrook, G., Borchelt, D., Iwatsubo, T., Sisodia, S. and Malinow, R. (2003) APP processing and synaptic function. *Neuron*, **37**, 925–937.
72. Koo, E.H. and Squazzo, S.L. (1994) Evidence that production and release of amyloid β-protein involves the endocytic pathway. *J. Biol. Chem.*, **269**, 17386–17389.
73. Kim, S.H., Leem, J.Y., Lah, J.J., Slunt, H.H., Levey, A.I., Thinakaran, G. and Sisodia, S.S. (2001) Multiple effects of aspartate mutant presenilin 1 on the processing and trafficking of amyloid precursor protein. *J. Biol. Chem.*, **276**, 43343–43350.
74. Kaether, C., Lammich, S., Edbauer, D., Ertl, M., Rietdorf, J., Capell, A., Steiner, H. and Haass, C. (2002) Presenilin-1 affects trafficking and processing of betaAPP and is targeted in a complex with nicastrin to the plasma membrane. *J. Cell Biol.*, **158**, 551–561.
75. Leem, J.Y., Saura, C.A., Pietrzik, C., Christianson, J., Wanamaker, C., King, L.T., Veselits, M.L., Tomita, T., Gasparini, L. and Iwatsubo, T. (2002) A role for presenilin 1 in regulating the delivery of amyloid precursor protein to the cell surface. *Neurobiol. Dis.*, **11**, 64–82.
76. Gravina, S.A., Ho, L., Eckman, C.B., Long, K.E., Otvos, L., Jr Younkin, L.H., Suzuki, N. and Younkin, S.G. (1995) Amyloid β protein (Aβ) in Alzheimer's disease brain. *J. Biol. Chem.*, **270**, 7013–7016.
77. Yamamoto, T. and Hirano, A. (1986) A comparative study of modified Bielschowsky, Bodian and thioflavin S stains on Alzheimer's neurofibrillary tangles. *Neuropathol. Appl. Neurobiol.*, **12**, 3–9.
78. Hirano, A. and Zimmerman, H.M. (1962) Alzheimer's neurofibrillary changes. A topographic study. *Arch. Neurol.*, **7**, 227–242.
79. Reaume, A.G., Howland, D.S., Trusko, S.P., Savage, M.J., Lang, D.M., Greenberg, B.D., Siman, R. and Scott, R.W. (1996) Enhanced amyloidogenic processing of the β-amyloid precursor protein in gene-targeted mice bearing the Swedish familial Alzheimer's disease mutations and a "humanized" Aβ sequence. *J. Biol. Chem.*, **271**, 23380–23388.
80. Slunt, H.H., Thinakaran, G., von Koch, C., Lo, A.C.Y., Tanzi, R.E. and Sisodia, S.S. (1994) Expression of a ubiquitous, cross-reactive homologue of the mouse β-amyloid precursor protein (APP). *J. Biol. Chem.*, **269**, 2637–2644.